PETROLEUM EXPLORATION AND DEVELOPMENT
Volume 48, Issue 4, August 2021
http://www.sciencedirect.com/journal/petroleum-exploration-and-development

Available online at www.sciencedirect.com
ScienceDirect

Cite this article as: PETROL. EXPLOR. DEVELOP., 2021, 48(4): 864–876.

RESEARCH PAPER

Genesis of calcite vein in basalt and its effect on reservoir quality: A case study of the Carboniferous in the east slope of Mahu sag, Junggar Basin, NW China

XIA Lu[1], CAO Yingchang[1, *], BIAN Baoli[2], LIU Hailei[2], WANG Xiaoxue[3], ZHAO Yiwei[1], YAN Miaomiao[1]

1. Key Laboratory of Deep Oil and Gas, China University of Petroleum (East China), Qingdao 266580, China;
2. Research Institute of Petroleum Exploration and Development, PetroChina Xinjiang Oilfield Company, Karamay 834000, China;
3. Research Institute of Petroleum Exploration and Development, PetroChina Tarim Oilfield Company, Korla 841000, China

Abstract: The characteristics and genesis of the calcite veins in Carboniferous basalt in the east slope of Mahu Sag, Junggar Basin are investigated based on observation of cores and thin sections; analyses of X-ray fluorescence, in situ major, trace and rare earth elements (REE), carbon, oxygen and strontium isotopes, fluid inclusions, as well as basin modeling. There are three periods of calcite fillings. The Period I calcite is characterized by low Mn content, flat REE pattern, strong negative cerium (Ce) anomaly, weak to moderate negative Eu anomaly, and light carbon isotopic composition, indicating the formation of the calcite was affected by meteoric water. The Period II calcite shows higher Mn and light REE contents, weak positive Ce anomaly and slight positive europium (Eu) anomaly, and a little heavier carbon isotopic composition and slightly lower strontium isotope ratio than the Period I calcite, suggesting that deep diagenetic fluids affected the formation of the Period II calcite to some extent. The Period III calcite is rich in iron and manganese and has REE pattern similar to that of the Period II calcite, but the cerium and europium enomalies vary significantly. The Period I and II calcites were formed in shallow diagenetic environment at approximately 250–260 Ma, corresponding to Late Hercynian orogeny at Late Permian. The Period III calcite was probably formed in the Indo-China movement during Late Triassic. It is believed that the precipitation of calcite in basalt fractures near unconformity was related to leaching and dissolution of carbonates in the overlying Lower Permian Fengcheng Formation by meteoric water, which destructed the Carboniferous weathering crust reservoirs in early stage. Relatively high quality reservoirs could be developed in positions with weak filling and strong late dissolution, such as structural high parts with Fengcheng Formation missing, distant strata from Fengcheng Formation vertically, buried hills inside lake basin, etc.

Key words: Junggar Basin; Mahu Sag; Carboniferous; calcite vein; geochemical characteristics; fluid source; reservoir quality

Introduction

Abundant oil and gas resources have been discovered in the Carboniferous volcanic rocks around Mahu Sag of the Junggar Basin, which have great exploration potential[1–3]. Volcanic rock fractures in the east slope of Mahu Sag (Madong area for short) are filled with calcite, causing poor reservoir quality. The genesis mechanism and distribution law of calcite veins are one of the key problems restricting oil and gas exploration in this area. The fluid activity in sedimentary basin is very important to reservoir diagenesis and reworking and is an important factor affecting reservoir quality[4–11]. In different stages of basin evolution, the fluid flow in fractures is usually presented as vein mineral occurrence[12–14]. Among them, calcite veins are more common, which are important records of fluid sources and geochemical evolution during thermal-tectonic evolution of sedimentary basins[8–10, 15]. The previous studies on the periphery of Mahu Sag mostly focused on the west and south of the sag. Moreover, there was a lack of detailed research on the characteristics and genesis of calcite filling in fractures in different periods[10–11, 16–17]. The calcite veins of the Carboniferous basalt reservoir in Madong area are taken as the main research objects in this study. Integrating the anal-

Received date: 30 Oct. 2019; **Revised date:** 20 May 2021.
*** Corresponding author.** E-mail: caoych@upc.edu.cn
Foundation item: Supported by the NSFC Innovative Research Group on Oil and Gas Accumulation Mechanism (41821002); Major Science and Technology Project of PetroChina (2017E-0401); China Postdoctoral Science Foundation (2019M662465).
https://doi.org/10.1016/S1876-3804(21)60072-1

analyses of mineral petrography, X-ray fluorescence (XRF), in-situ micro-elements, O-, C- and Sr-isotope composition, fluid-inclusion homogenization temperature, and basin modeling, we clarify the geochemical characteristics and formation periods of calcites in different stages, reveal the evolution characteristics of diagenetic fluids, and discuss the effect of calcite filling on reservoir quality, so as to point out the direction of favorable reservoir prediction.

1. Geological setting

The study area is located on the east of the Mahu hydrocarbon-rich sag in the northwestern margin of the Junggar Basin, and is a southwest dipping monoclinal structure developed from the Hercynian Movement (Fig. 1). Three large nose-shaped salients are developed from north to south in Madong area, all extending tens of kilometers towards Mahu Sag, so the structural conditions are good. Several large anticlines are locally developed, forming inherited positive structures that are favorable for petroleum migration and accumulation[3]. Deep Carboniferous igneous rocks are mainly intermediate-basic volcanic rocks[3], which have experienced the Hercynian, Indosinian, Yanshanian and Himalayan tectonic movements[18–23]. Under the influence of weathering and leaching, compaction, dissolution, filling, recrystallization and other diagenesis, the reservoir space is dominated by fractures and secondary dissolved pores, with fewer primary pores[3]. The Carboniferous is in unconformable contact with the overlying strata, and the Permian overlap pinch-out is obvious in the middle of the nose-shaped salient structural belt. Oil and gas shows are

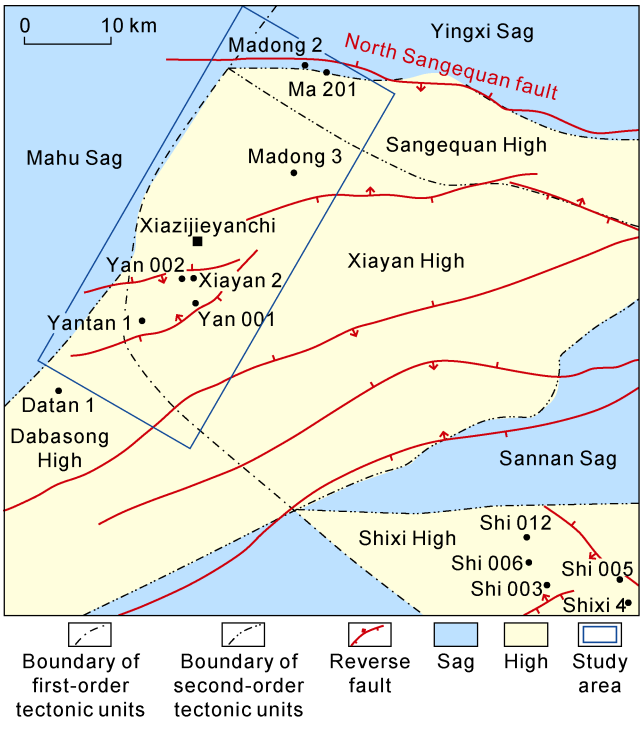

Fig. 1. Geological structures in the study area.

detected in the Carboniferous, Permian, Triassic and Jurassic System, mainly from the source rocks of the Lower Permian Fengcheng Formation in Mahu Sag[24]. In Well Madong 3 and Well Xiayan 2, oil and gas shows are discovered in the Carboniferous, which is presented mainly as oil-bearing beds and oil-water beds. Compared with the Shixi oilfield on the Shixi high in the southeast, the reservoir size is smaller. Well Datan 1 in the south was drilled to a depth of 6 226 m, with a total of 35 m in 3 layers of abnormal gas logging. No oil and gas show was detected in Well Ma 201 in the north.

2. Materials and methods

Most of the Carboniferous volcanic rock cores in Madong area are basalt, and a small amount of andesite and tuff are developed locally. The Bruker M4 Tornado micro-X-ray fluorescence spectrometer was used for elemental analysis of the rock samples. In order to clarify the differences in chemical composition and spatial distribution of calcites in different stages, the favorite parts with larger thickness of the veins in representative samples were selected for emphasis analysis.

XRF, conventional rock section, fluorescence and cathodoluminescence analyses, and homogenization temperature of fluid inclusions were performed in the key laboratory of deep oil and gas in China University of Petroleum (East China). The indoor temperature was 23 °C and the relative humidity was 50%. Each polished sample was tested by XRF for more than 8 h, with a resolution of 40 μm. The X-ray voltage and current were 50 kV and 600 μA, respectively. The qualitative and quantitative characteristics of Na, K, Al, Si, Mg, Ca, Fe, Co, Mn, S, Sr, Ti, V, and Ba were detected. On this basis, the optical, fluorescence and cathodoluminescence identification of the thin sections were carried out by means of ZEISS Axio Imager A2 microscope and CL8200MK5 cathodoluminescence instrument. The homogenization temperature of 17 fluid inclusions in representative calcite vein samples was measured by using a ZEISS microscope equipped with a LINKAM THMS600 stage, and temperature measurement error is ±0.1 °C.

In-situ major and trace elements and Sr isotopic analysis of thin sections were determined at State Key Laboratory of Ore Deposit Geochemistry in Guiyang Institute of Geochemistry, Chinese Academy of Sciences. Elemental analysis devices included GeoLasPro laser-ablation system and Agilent 7700x inductively coupled plasma mass spectrometry (ICP-MS) instrument, and the beam spot diameter was 50 μm. The international standards NIST SRM 610 and NIST SRM612 were used as external calibration. Multiple external standards and no internal standard methods were used for quantitative calculation, and ICPMSDataCal software was used to perform the offline data processing[25]. On the basis of major and

trace element analysis, the locations with relatively high Sr content in the sample were selected. In-situ Sr isotopic ratio was determined by using the above mentioned laser-ablation system in combination with the Neptune Plus multi-receiver inductively coupled-plasma mass spectrometer (MC-ICP-MS). The beam spot with diameter of 180 μm was used because the content of Sr in calcite veins is low. Coral-1 was used as the standard sample, and a mean value of 0.709 175±0.000 05 was obtained.

Microdrilling of calcite thin sections and oxygen and carbon isotopic composition tests of Well Ma 201 were performed at the State Key Laboratory of Geological Processes and Mineral Resources, China University of Geosciences (Wuhan). The powder samples of two-period calcites in fractures were obtained using a microscope fitted with a 100 μm diameter microdrill system. The samples were reacted with 100% pure phosphoric acid in vacuum and then separated from the acid for 4 h at 25 °C using the chemical separation method proposed by Al-Aasm et al.[26]. The isotopic ratios of the generated CO_2 were analyzed by means of MAT-253 gas isotope mass spectrometer. Both $\delta^{13}C$ and $\delta^{18}O$ values were measured by taking PDB as the standard and the measurement error was less than 0.2‰. Six calcite samples were drilled from volcanic fractures under hand specimen scale by using the small bit and ground into powder. By means of the above method, carbon and oxygen isotopes were tested at the Institute of Geology and Geophysics, Chinese Academy of Sciences.

3. Characteristics and filling periods of calcite veins

3.1. Fracture characteristics and filling compositions

The buried depth of most Carboniferous basalt reservoirs in Madong area is more than 3500 m. There are a lot of structural fractures in the core (Figs. 2 and 3). For example, there is one high-angle (70°–80°) fracture and two low-angle fractures developed in the basalt of Well Ma 201 at a depth of 3877.13 m (Fig. 2a). The wells with high fracture density are mainly located near the main controlling fault (Figs. 1 and 4a). For example, the average linear density of core fractures in Well Yan 001 which is closer to the main controlling fault is 4.7 fractures·m^{-1}, whereas that in Well Madong 3 which is farther from the main controlling fault is 1.9 fractures·m^{-1}. According to the observation results, there are 52 fully filled, 17 semi-filled and 11 unfilled fractures in the basalt cores, accounting for 65.00%, 21.25% and 13.75% of the total, respectively (Fig. 4b). The fractures are filled mainly by calcite, which bubbles violently with the drops of dilute hydrochloric acid.

The brighter the color is, the higher the relative content in the monochromatic diagram of XRF elemental analysis (Fig. 3). At the depth of 3877.13 m in Well Ma 201, fractures and pores inside the basalt do not contain Ti, whereas the surrounding rock contains Ti and Ti enrichment strips appear locally. The dislocation of Ti-rich strips indicates that the high-angle fracture is a micro reverse fault with a vertical fault distance of less than 1 cm (Fig. 3a). Ca is relatively enriched in pores and fractures (Fig. 3b). The distribution of Mn is similar to that of Ca but relatively limited, and mainly occupies the horizontal fractures and parts of the fault between the horizontal fractures (Fig. 3c). At the depth of 4678.90 m in Well Madong 3, the basalt fractures have large opening, in which the width of calcite vein filling is up to 8 mm (Fig. 3d). There are differences in the composition of calcite veins, which are mainly manifested in different Mn

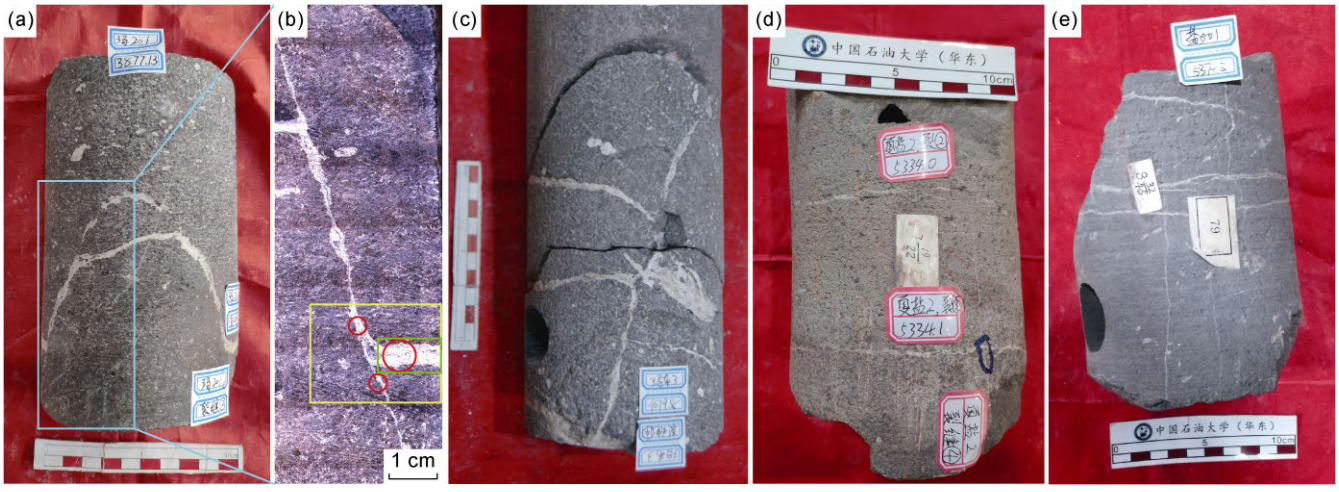

Fig. 2. Characteristics of core fractures in Madong area (blue box: sample cutting position; yellow box: position of thin section; red circle: position of microzone test; green box: micro-drilling position at the thin-section scale). (a) At 3877.13 m in Well Ma 201, two low-angle fractures and one high-angle fracture, calcite filling; (b) cross-section photograph of the core sample in Fig. (a) after cutting; (c) at 4679.80 m in Well Madong 3, high-angle fracture and low-angle fractures, calcite filling; (d) at 5334.10 m in Well Xiayan 2, horizontal fractures and vertical fractures, calcite filling; (e) at 5374.50 m in Well Yan 001, vertical fractures terminating near horizontal or low-angle fractures, calcite filling.

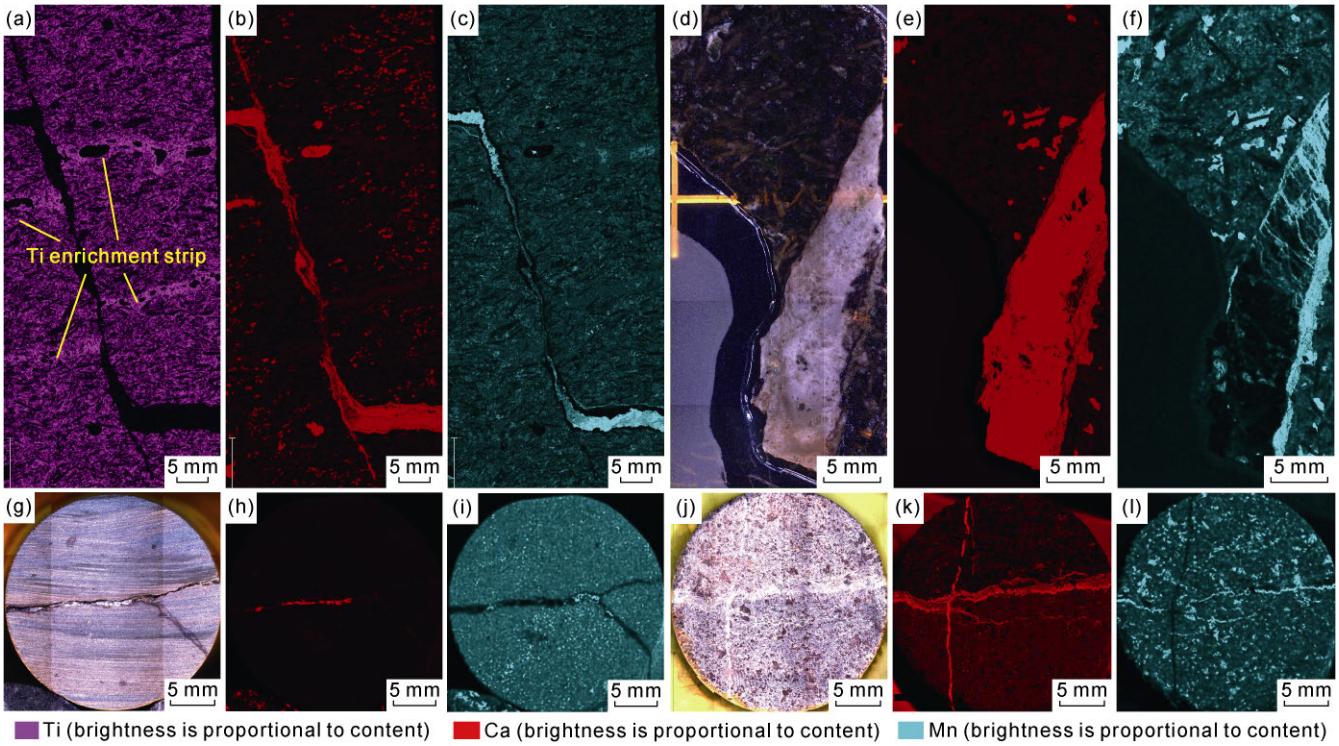

Fig. 3. XRF scanning results of core samples in Madong area. (a) At 3877.13 m in Well Ma 201, basalt, Ti content distribution, bright Ti-rich strips are dislocated, see the photo of the corresponding rock sample in Fig. 2b; (b) at 3877.13 m in Well Ma 201, Ca content distribution, Ca is rich in fractures and pores; (c) at 3877.13 m in Well Ma 201, Mn content distribution, Mn is rich in fractures; (d) at 4678.90 m in Well Madong 3, photo of basalt sample; (e) at 4678.90 m in Well Madong 3, Ca content distribution, Ca is rich in fractures and pores; (f) at 4678.90 m in Well Madong 3, Mn content distribution, the distribution of Mn is irregular and the fracture edge is relatively rich in Mn; (g) at 4634.70 m in Well Madong 3, photo of andesite sample; (h) at 4634.70 m in Well Madong 3, Ca content distribution, Ca is rich locally in fractures; (i) at 4634.70 m in Well Madong 3, Mn content distribution, the distribution of Mn is limited in the fractures; (j) at 5334.10 m in Well Xiayan 2, photo of basalt sample, the sampling location is shown in Fig. 2d; (k) at 5334.10 m in Well Xiayan 2, Ca content distribution, Ca is rich in fractures; (l) at 5334.10 m in Well Xiayan 2, Mn content distribution, Mn is rich in lower part of horizontal fractures.

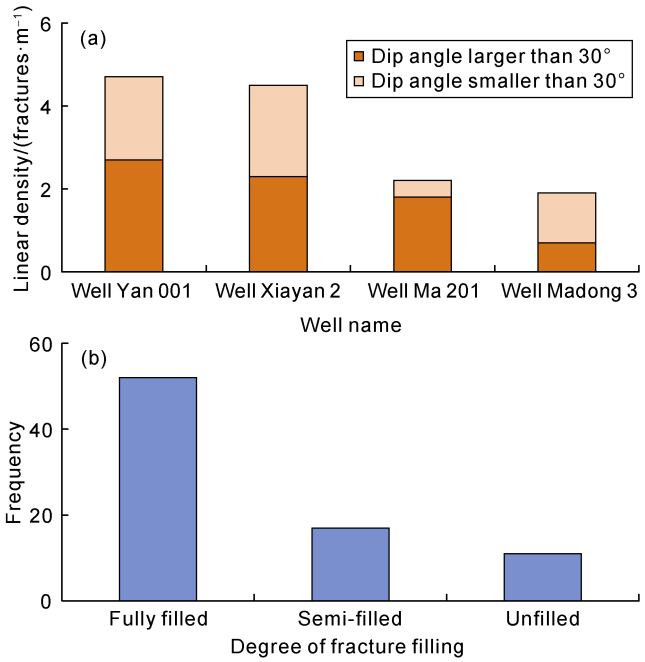

Fig. 4. Histograms of core fracture density (a) and filling degree (b) in Madong area.

content (Fig. 3e, 3f). At the depth of 4634.70 m in Well Madong 3, there are two intersecting fractures in andesite, one of which does not contain Ca, while the other is partially filled with calcite and has a lower Mn content (Fig. 3g–3i). At the depth of 5334.10 m in Well Xiayan 2, one narrow vertical fracture and one wide horizontal fracture are developed in the basalt, both of which are filled with calcite (Fig. 3j, 3k). Vertical calcite veins are almost free of Mn, while the upper part of horizontal veins is poor in Mn and the lower part is rich in Mn (Fig. 3l). The superposition diagram of Ca and Mn shows that there are two periods of different fillings in the same horizontal vein in the samples of Well Ma 201 (Fig. 5a), which are located on the edge and inside of the pores and fractures respectively (Fig. 5a①). The lower horizontal vein is wider and obviously different in the two-period fillings (Fig. 5a②), so it is selected as the key research site. The Ca content in green fillings accounts for 97.8% of the total contents of the nine elements analyzed. The contents of other elements are all lower than 1.0%, and the content of Mn is very low (Fig. 5b). For the red fillings, Ca content accounts for 91.7%, Mn and Si contents are 4.0% and 2.5%, respectively, but Mg and Cl contents are very low (Fig. 5b).

3.2. Petrographic characteristics and filling periods of the typical calcite veins

Mineral crystal characteristics at different positions of

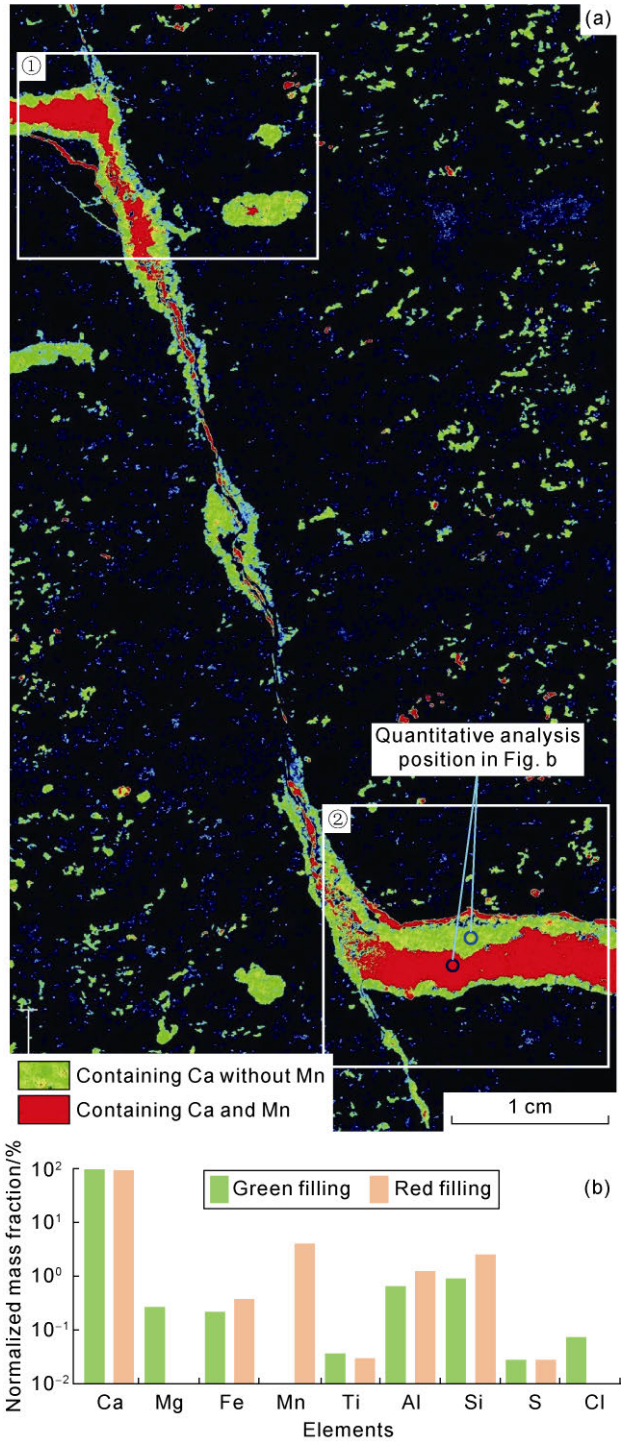

Fig. 5. XRF scanning two-element superposition chart (a) and element content histogram (b) of core samples in Well Ma 201.

horizontal calcite veins in Well Ma 201 are different (Fig. 6). The calcite at the edge of the veins in contact with surrounding rocks is blade-like, serrated or horse-tooth shaped. Their idiomorphic degree is better, and most calcites are idiomorphic–hypidiomorphic middle-coarse crystals. Larger crystals are locally developed and grow mainly perpendicular to the fracture wall, with obvious cleavage, clean surface, no cathodoluminescence and early forming time (Fig. 6a–6c). The crystals far from the fracture wall in the middle of the vein are generally larger in size and dominated by idiomorphic–hypidiomorphic granular coarse or very coarse crystals, with one or two groups of cleavages, clean surface, maroon cathodoluminescence and late forming time (Fig. 6a–6c). The calcites show poor idiomorphism with maroon cathodoluminescence near and inside the high-angle fractures and in the upper associated veinlets. Some of these calcites have rough surfaces. Calcite crystals are associated with chlorite and other minerals inside high- angle fractures. In addition, chlorite is developed near the boundary of two periods of calcites with different cathodoluminescence characteristics in the horizontal vein (Fig. 6d, 6e).

Three periods of calcite fillings are developed in the basalt fractures in the study area (Fig. 6f, 6g). The Period-I calcite is poor in Mn and does not show cathodoluminescence. It is light blue fluorescence near the fracture wall and yellow brown fluorescence at the fracture edge. The Period-II calcite is rich in Mn, the cathodoluminescence is maroon and the fluorescence is not obvious. The Period-III calcite intermittently fills in small irregular fractures and is associated with orange fluorescent substances.

4. Genesis of calcite vein in basalt

4.1. Fluid source

Microscopic characteristics and geochemical data indicate that the calcites in different periods in the study area derived from the fluids with different compositions and origins.

Period-I calcite vein is the earliest calcite precipitated after fracture opening, and grows mainly perpendicular to fracture wall which is generally formed by fracture opening-closing mechanism[27]. Fluorescence bands are developed locally adjacent to the fracture wall at the top, and the calcites near the fracture wall at the bottom show weak fluorescence and no fluorescence bands (Fig. 6f). Fluorescence bands reveal the periodic growth of calcite, which may be related to the seasonal variation of organic matter in water or the episodic oil-gas charging. Previous studies indicate that episodic oil-gas charging in the western Mahu Sag of the Junggar Basin could result in the formation of circular fluorescent calcite cements[8–9]. However, fluorescent oil and gas inclusions are not discovered in the veins of Period-I calcite in Madong area. The right-dipping distribution pattern of rare earth elements (REE) of calcite vein derived from diagenetic and hydrocarbon fluids[28] are different from those of flat REE pattern of Period-I calcite vein. Therefore, Fluorescence bands in Period-I calcite veins are likely to be irrelevant with oil and gas charging. The three-terminal chart of Mg, Fe and Mn contents shows that Period-I calcite is characterized by high Mg, low Fe and ultra-low Mn

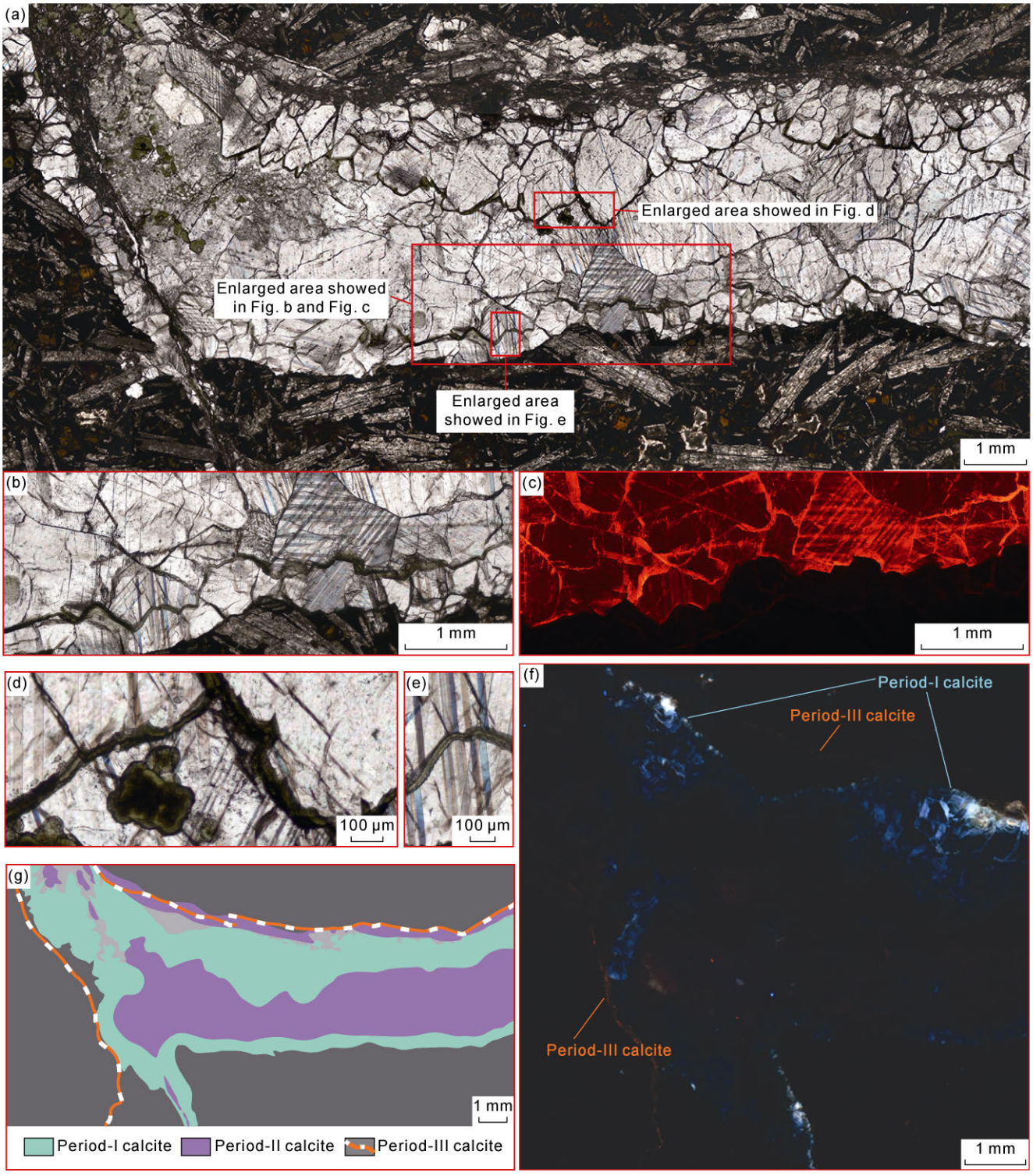

Fig. 6. Microscopic characteristics and filling periods of calcite veins in core sample from Well Ma 201. (a) 3877.13 m, calcite veins in basalt, plane-polarized light; (b) Horse-tooth shaped calcites with small crystal size are located in the lower margin of the vein with cleavage developed locally while the calcites with relatively larger crystal size and obvious cleavages are developed inside the vein, plane-polarized light; (c) Calcites in the lower margin of the vein show no cathodoluminescence whereas those inside the vein are maroon, cathodoluminescence; (d) (e) Chlorite can be discovered near the boundary between the two periods of calcites, plane-polarized light; (f) It is light blue fluorescence at the edge of the thick veins and tawny locally along the margin. Irregular veinlets show intermittent orange fluorescence, ultraviolet fluorescence; (g) Schematic distribution of three periods of calcite fillings.

(Figs. 5, 7 and 8). It was previously deemed that the calcites of fresh-water origin in limestone fractures in the Lower Paleozoic of the Ordos Basin, NW China and in the Permian of Jingshan area, Mid-Yangtze are lack of Fe and Mn compounds[29]. Therefore, it can be inferred that Period-I calcite might be affected by fresh water during its precipitation.

Total REE contents of typical calcite veins in Well Ma

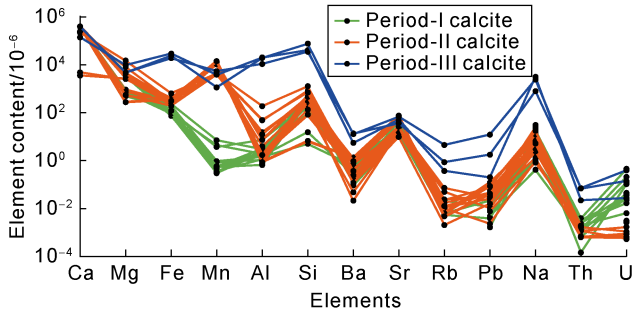

Fig. 7. Distribution of contents of major and trace elements of calcite vein in Well Ma 201.

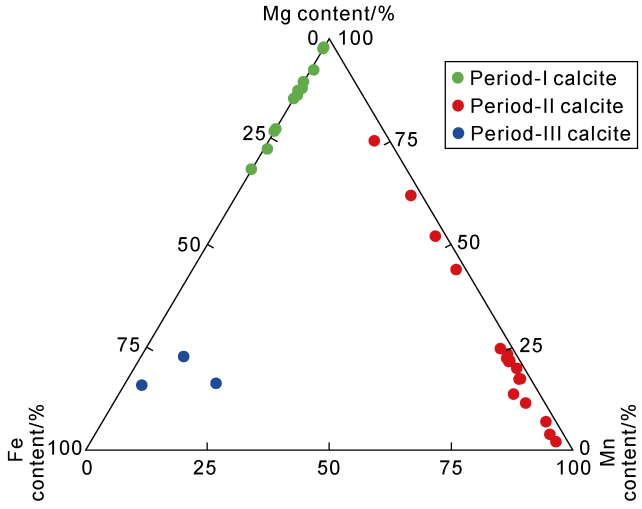

Fig. 8. Three-terminal chart of Mg, Fe and Mn contents of vein calcite in Well Ma 201.

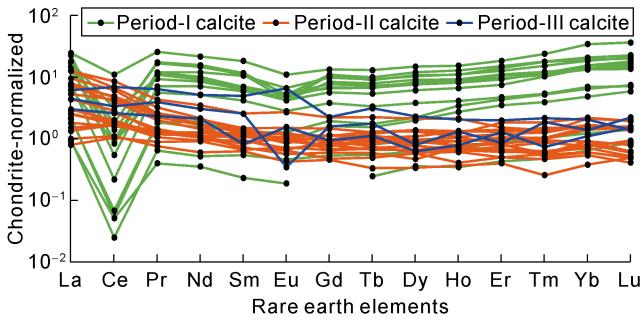

Fig. 9. Chondrite-normalized-REE patterns of vein calcite in Well Ma 201.

201 are (1.27–71.93)×10^{-6}, averaging 16.37×10^{-6}. The REE after being normalized on the basis of chondrite[30] presents significant differentiation in distribution (Fig. 9). The average value of chondrite-normalized La/Yb in Period-I calcite is 0.91, indicating that the differentiation of light rare earth (LREE) and heavy rare earth elements (HREE) is not obvious (Fig. 10a). Strong Ce negative anomalies and weak-moderate Eu negative anomalies (Fig. 10b) suggest that the calcites are precipitated in a strong oxidizing environment[28, 31]. The amplitude of Ce and Eu anomalies remain basically unchanged (Fig. 10b), indicating that fluid properties and diagenetic environment are relatively stable.

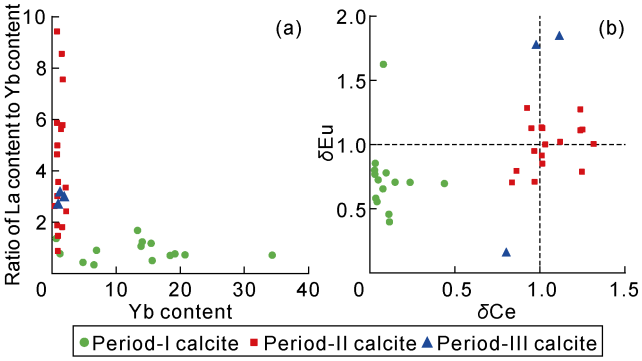

Fig. 10. Cross-plots of La and Yb (a) and Eu and Ce anomalies (b) of chondrite-normalized calcite veins in Well Ma 201.

Previous studies suggest that the carbon and oxygen isotopic compositions of the Carboniferous–Permian volcanic reservoirs in the northwestern margin of the Junggar Basin are relatively light, with the $\delta^{18}O$ of −23.6‰–−8.1‰ and $\delta^{13}C$ of −21.5‰–−3‰[8–11, 16]. The $\delta^{13}C$ of volcanic fracture-filling calcite in Madong area varies from −5‰ to −1‰, and the $\delta^{18}O$ ranges from −16‰ to −9‰ (Fig. 11a). Furthermore, as the distance from top unconformity surface increases, the carbon isotopic compositions tend to get heavier (Fig. 11b). The $\delta^{13}C$ of Period-I calcite sample at 3877.13 m of Well Ma 201 is −3.74‰, and that at 4637.50 m of Well Madong 3 is −4.07‰. The carbon isotopic composition of calcite formed under the influence of atmospheric fresh water generally ranges from −7.0‰ to −3.5‰[32–33]. The value of Period-I calcite in this paper is in this range, indicating that its formation process is affected by atmospheric fresh water.

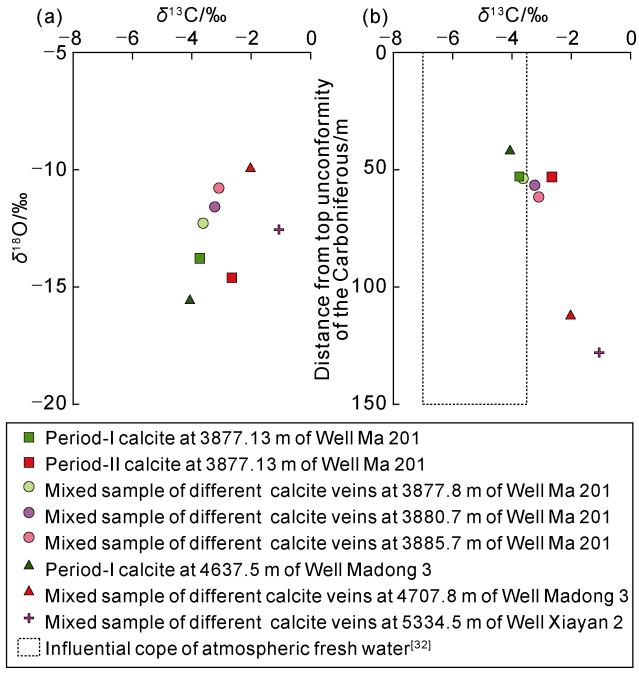

Fig. 11. Cross-plot of carbon and oxygen isotopic compositions (a) and vertical distribution of carbon isotopic composition (b) of calcite veins in Madong area.

It can be concluded that Period-I calcite is formed in a relatively oxidized diagenetic environment, and its precipitation process is always affected by atmospheric fresh water. In volcanic strata, open faults and relatively open environment are formed easily under the action of tectonic stress. The formation water in fractures communicates with the atmospheric fresh water near the surface, which makes the atmospheric water participate in calcite precipitation and diagenesis.

Period-II calcite is formed after Period-I, and it is wider. The crystals in the vein bodies are coarser with good idiomorphic degree, whereas those in veinlets and high-angle veins are mainly anidiomorphic (Fig. 6). Period-II calcite shows higher contents of Fe and Mn (Figs. 7, 8 and 12). The interaction between the formation fluid and volcanic material could increase the contents of Fe and Mn in the fluid. This water-rock interaction may be the weathering and leaching near ground surface[7–8, 34], or the deep buried water-rock reaction under high temperature and pressure[6, 8]. The REE of Period-II calcite veins is in the pattern right-dipping distribution (Fig. 9) and most samples present obvious enriched LREE patterns, weak–moderate Ce positive anomalies and weak Eu positive anomalies (Fig. 10b), showing the characteristics of calcite of hydrothermal origin to some degree[35]. The test results of carbon and oxygen isotopic compositions also indicate that the formation of Period-II calcite is not affected by atmospheric fresh water (Fig. 11), but related to burial diagenetic fluids. Strontium isotope ratios are in the range of 0.703–0.705 (Fig. 13), showing the characteristics of deep-source fluids, which is probably caused by the interaction of deep fluid with volcanic material in the process of its upwelling[8].

To sum up, Period-II vein calcite is formed in a burial diagenetic environment unaffected by atmospheric fresh water, influenced by deep diagenetic fluid to some degree. During the evolution of the vein-forming fluid, Fe, Mn and other metallic elements are enriched gradually and REEs get depleted gradually (Fig. 12).

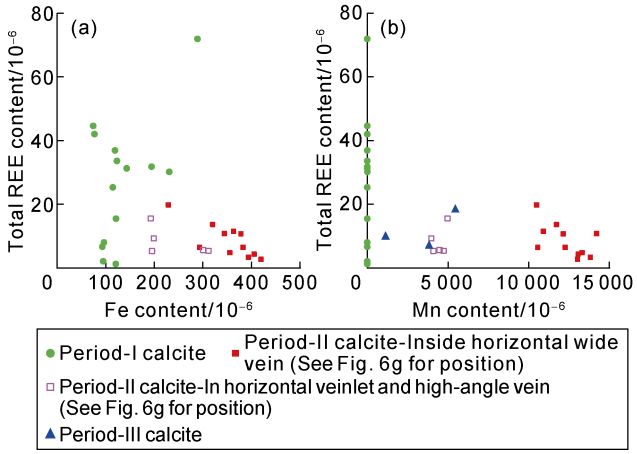

Fig. 12. Cross-plots of total REE content with Fe (a) and Mn (b) contents of calcite vein in Well Ma 201.

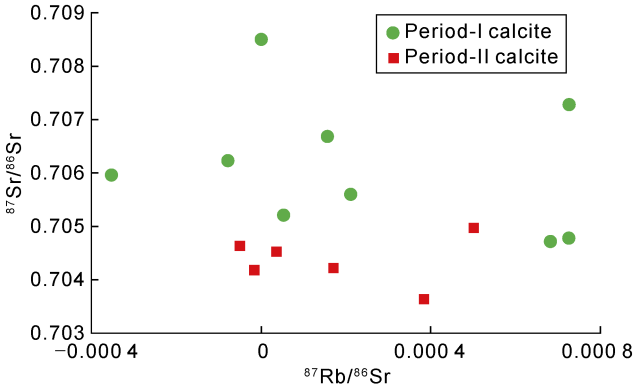

Fig. 13. Cross-plot of strontium isotope ratios of calcite vein in Well Ma 201.

The Period-III calcite mainly extends along the edge of the first two periods of veins and is obviously controlled by the distribution of early veins, and its forming time is the latest (Fig. 6g). Period-III calcite shows no fluorescence by itself, but is associated with orange fluorescent materials. Calcite is discontinuously distributed in fractures and the space between disconnected calcite veins is occupied by suspected hydrocarbon substance with orange fluorescence. The test signals of the in-situ micro-area at three measurement points are poor because the fillings of Period-III are so narrow and affected by the orange fluorescent materials inside the vein bodies or the surrounding rocks. The Mn content of Period-III calcite is close to that of some measurement points in Period-II calcite (Fig. 12b). The contents of Fe, Mg, Al, Si and Na are significantly higher than those of the other two periods (Figs. 7 and 8), which may be caused by ferro-magnesium minerals and albite in the basalt near the fracture. The REE distribution pattern of Period-III is right-dipping (Fig. 9), characterized by LREE enrichment, insignificant Ce anomalies and large fluctuation of Eu anomalies (Fig. 10b).

4.2. Tectonic activity and formation of vein

Bounded by the top surface of the Triassic, Madong area is vertically divided into a shallow fault system dominated by normal faults and a deep fault system dominated by reverse faults[20]. Nearly EW trending reverse faults are developed in the north of study area, and NEE-SWW trending reverse faults are developed in the south (Fig. 1). The formation and evolution of faults are mainly influenced by the compression stresses of late Hercynian and Indosinian, characterized by compressional torsion and strike-slip[21–23]. The northwestern margin of Junggar Basin entered the stage of dextral compression-shearing strike-slip thrusting in the late Permian, leading to uplift and denudation in the northern part of the basin[22–23]. Madong area is near the center part of the basin and accepted the deposits of a set of proximal fan-deltaic conglomerate strata in the Middle

Permian. The range of fault activity in the Late Permian was smaller than that in the west of Mahu Sag. Although the thrust structure was not developed, parts of the Middle and Upper Permian were still missing.

No fluorescent inclusions are discovered in Period-I and Period-II calcite veins at the depth of 3877.13 m in Well Ma 201, whereas brine inclusions without fluorescence are developed (Fig. 14). No fluid inclusions are discovered in the veinlets of Period-III calcite. The inclusions homogenization temperatures of Period-I and Period-II calcite veins are very close (Table 1). Homogenization temperature of Period-I calcite vein ranges from

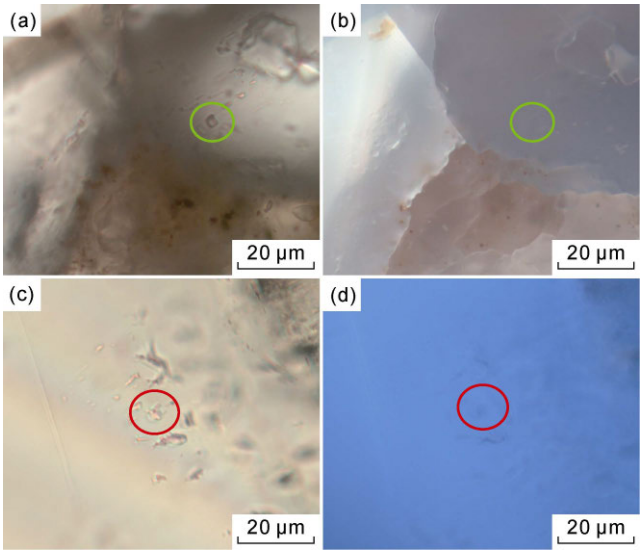

Fig. 14. Characteristics of brine inclusions of calcite veins in basalt samples from Well Ma 201. (a) and (b) are the plane-polarized and fluorescent photos in the same field of view. The green circle indicates the location of the inclusion in Period-I calcite. (c) and (d) are the plane-polarized and fluorescent photos in the same field of view. The red circle shows the location of the inclusion in Period-II calcite.

Table 1. Test results of homogenization temperatures of brine inclusions in basalt calcite vein at 3877.13 m in Well Ma 201.

Period of host calcite	Inclusion No.	Diameter/ μm	Homogenization temperature/°C
Period-I	A1	6.6	85.2
	A2	4.2	84.7
	A3	5.3	86.1
	A4	5.8	92.6
	A5	4.1	81.7
	A6	4.8	86.8
	A7	5.5	80.7
Period-II	B01	5.1	90.8
	B02	6.8	91.2
	B03	7.7	96.7
	B04	6.5	82.7
	B05	7.5	77.2
	B06	5.9	80.8
	B07	8.0	89.1
	B08	5.5	88.2
	B09	12.4	86.9
	B10	6.0	76.5

80.7 °C to 92.6 °C, with the average of 85.4 °C, while that of Period-II varies from 76.5 °C to 96.7 °C, and the average value is 88.3 °C excluding the two abnormal low-temperature values less than 80 °C, which was slightly higher than that of Period-I.

Single-well burial history and thermal history were simulated based on the research results of burial history in Well Yantan 1[36] and strata erosion thickness by Zhou et al.[37] and thermal history of Well Madong 2[38]. The Hercynian weathering and leaching time of the Carboniferous system in the Shixi high in the southeast is longer, whereas the uplifting and erosion time in Madong area is shorter (Fig. 15). The tested peak homogenization temperatures of inclusions in Period-I and Period-II calcites at the depth of 3877.13 m in Well Ma 201 are in the range of 85–90 °C, corresponding to the fluid activity time of mainly 250–260 Ma and burial depth of 500–700 m (Fig. 15). The vein forming time based on homogenization temperature is consistent with the geological age of Hercynian Movement. The low-angle fractures which can be closed easily under overburden loads cannot form calcite veins unless they are filled in time. For this, tectonic compression, fracture opening, fluid activity and calcite filling shall be roughly simultaneous. The Period-I and Period-II calcites were mainly formed during the Late Hercynian Movement at the end of the Permian. The deep reverse fault cutting through the top surface of the Carboniferous in Madong area mainly breaks the Triassic and the strata below, indicating that the fault activity mainly occurred during the Hercynian and the Indosinian[20]. These reverse faults have large fault displacements and long extensions, which control the development of the nose-shaped salient structure in this area. The North Sangequan fault is the boundary fault of the nose-shaped salient structure of Well Madong 2 (Fig. 1). The plane extension distance of the fault is up to 50 km, and the fault displacement at the top Carboniferous in Well Ma 201 is approximately 300 m. The Permian–Triassic reservoirs in Madong area have received two periods of oil and gas charging, namely mature oil in the Late Triassic and highly mature oil in the Early Cretaceous[24, 39]. According to the strata cut by faults and fluorescence color in calcite veins, it is suggested that Period-III veinlets were probably formed in the Late Triassic. The genesis of the calcite vein in the basalt near the unconformity is related to the carbonate composition of the overlying strata leached by atmospheric fresh water (Fig. 11b). The direct overlying strata of the Carboniferous in the west and south of Madong area is the Fengcheng Formation of Lower Permian, and argillaceous limestone and marl are developed in the Fengcheng Formation of Well Yantan 1 and Xiayan 2, respectively. The fluid generated from mature organic matter has little effect on the formation of the first two periods of calcites, but it is likely to affect the formation of Period-III veinlets.

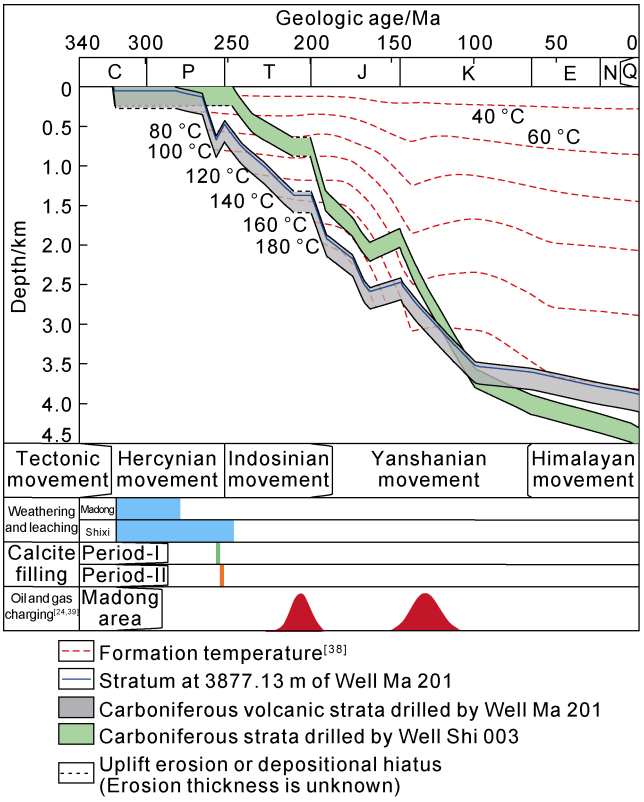

Fig. 15. Comparison of single-well burial history and timing of key diagenetic events in Madong and Shixi areas.

5. Effect of calcite filling on reservoir quality

Weathering and leaching as well as dissolution are constructive diagenesis for Carboniferous volcanic reservoirs in Madong area, whereas filling is destructive diagenesis, especially the filling of the first two periods of calcite. Fully filled and semi-filled fractures of calcite in cores account for approximately 86% (Fig. 4b). The Period-I calcite filling mainly destroys primary pores and small-opening fractures, whereas the Period-II calcite filling mainly destroys large-opening fractures (Fig. 5). Compared with the volcanic weathering crust reservoir of Shixi high in the southeast of the study area, the volcanic reservoirs at the top of Carboniferous in Madong area are poorer in physical properties, where primary pores, secondary pores and microfractures are mostly filled with calcite and the reservoir porosity within 50 m away from the unconformity is usually less than 4% (Fig. 16). The overlying strata of Carboniferous oil reservoir in Shixi high are the Middle and Lower Triassic, without the Permian including Fengcheng Formation. The uplift denudation time of volcanic rocks in this area is as long as 50 Ma, and the secondary dissolution pores and fractures without calcite filling are developed (Figs. 15 and 16). The Carboniferous in Madong area is overlain by the Middle and Lower Permian, and the carbonate-rich Fengcheng Formation directly overlaps the weathering crust, providing a large number of ions for calcite precipitation in the pores and fractures in underlying volcanic rocks. A lot of faults and fractures were developed during Late Hercynian Movement, along which atmospheric fresh water flowed into the Carboniferous formation water to form relatively oxidized diagenetic environment, so as to provide the condition for the precipitation of Period-I calcite. With the gradual weakening of the influence of atmospheric water, coupled with the deep water-rock reaction, the contents of Fe and Mn in formation water increased and the Period-II calcite further filled the residual pores and fractures.

Despite the adverse effects of early calcite filling, favorable reservoirs could be developed in the locations with weak filling degree or strong dissolution in later periods: (1) The Fengcheng Formation of Lower Permian in Mahu Sag thins towards northeast and gradually overlaps and pinches out at Xiayan high and Sangequan high in Madong area. In the structural highs without Lower Permian, particularly the positions missing the entire Permian, Carboniferous volcanic rocks undergoes weathering and leaching for a long time and is less influenced by the Fengcheng Formation, so the reservoirs with good physical properties could be developed. (2) Even though the carbonate-rich Fengcheng Formation is developed in the overlying strata, relatively high quality reservoirs can be also formed in the volcanic rocks far from the Fengcheng Formation vertically if it is laterally farther from faults controlled by the Hercynian with less intense deep fluid activity and relatively developed pores and fractures. When the depth from the top unconformity is greater than 50 m, higher-porosity zones appear locally in volcanic rocks (Fig. 16), and the carbon isotopic composition of calcite vein gradually moves away from the influence range of atmospheric fresh water (Fig. 11b), indicating that the influence range of calcite filling in vertical direction is limited. With the increase of the distance from the top unconformity, the degree of weathering and leaching decreases correspondingly. However, the reservoirs with good physical properties could still be developed far from the top surface of the Carboniferous. For one thing, the weathering and leaching of Carboniferous weathering crust around Mahu Sag had a large influence range vertically. For example, the influence depth of Zhongguai high in the southwest of Mahu Sag could reach 400 m[40]. For another, the interface between different eruption periods within the volcanic rocks is also an important control factor for the development of relatively high-quality reservoirs. During inactive eruption, the exposed volcanoes could be reworked by weathering and leaching. (3) The buried hills close to the high-quality source rocks inside the lacustrine basin and affected by strong dissolution in the late period are also favorable locations for the development of high-quality reservoirs. The source rocks of Fengcheng Formation overlie the Carboniferous volcanic rocks. The inherited

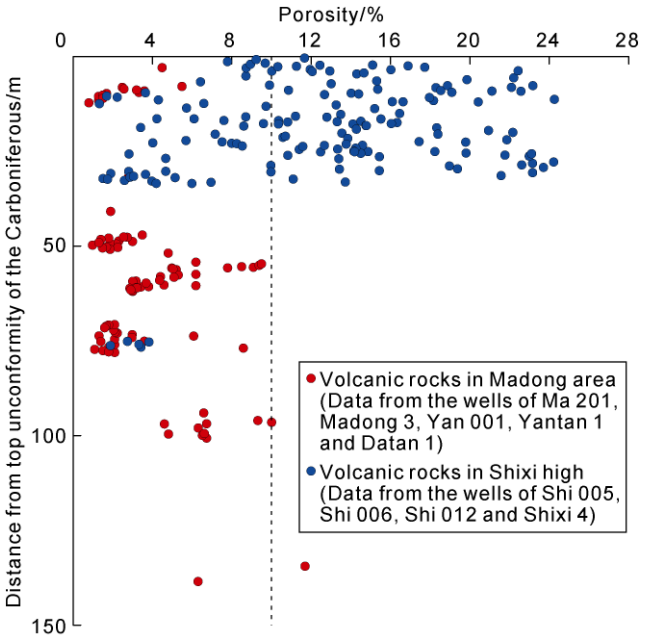

Fig. 16. Vertical distribution of porosity of Carboniferous reservoirs in Madong and Shixi areas.

buried hill near the central part of the basin is not only in contact with the source rock upward, but also in lateral connection with the high-quality source rock through faults, which is beneficial to the dissolution of acid fluid in the later stage. Even under the influence of early calcite filling, these buried hills are still potential sites for the development of favorable reservoirs.

6. Conclusions

The calcite veins in Carboniferous basalt in the east slope of Mahu Sag develop three periods of filling. Period-I calcite veins are mostly blade-like, serrated or horse-tooth shaped with high degree of idiomorphism, mostly idiomorphic–hypidiomorphic middle-coarse crystals. They mainly grow perpendicular to fracture wall, with no cathodoluminescence display and very low Mn content. They are precipitated early, formed in a relatively open diagenetic environment, and mainly originated from the atmospheric water leaching of the carbonate minererals from the overlying strata. Period-II calcite is rich in Mn with cathodoluminescence of maroon. The crystals in wide fractures are of high idiomorphism degree and dominated by idiomorphic–hypidiomorphic granular coarse or very coarse crystals with developed cleavages and clean surface, whereas those in narrow fractures show poor idiomorphism with relatively rough surfaces. The veins of this period are formed a little later than Period-Ⅰ and derived from burial diagenetic fluid, which are influenced by deep diagenetic fluid to some degree. During the growth of the calcite, the fluid gradually gets rich in Fe, Mn and other metal elements and depletes in rare earth elements. The Period-III calcite often fills in small irregular fractures and is associated with orange fluorescent materials. The locations of its development are usually controlled by the distribution of early fractures and veins, and its formation is the latest.

Period-I and Period-II calcites were generated during the Hercynian movement at the end of the Permian, filling most of the fractures and pores in the basalt reservoirs, so as to destroy the quality of the weathering crust reservoir at the top of the Carboniferous. The formation of Period-III calcite is probably related to the Indosinian movement during the Late Triassic, but it has less influence on the reservoir quality. The areas with weak calcite filling in early stage and strong dissolution in late stage are the potential sites for the development of favorable reservoirs. The formation of the calcite filling near the unconformity is mainly related to the carbonate composition of the overlying Fengcheng Formation in Lower Permian leached by atmospheric fresh water. High-quality reservoirs are developed in the structural highs where the Permian is missing. For the development area of Fengcheng Formation, relatively high-quality reservoirs are developed in the areas vertically far from the top unconformity of Carboniferous and in the buried hills inside the lake basin near the high-quality source rocks.

References

[1] HU Suyun, WANG Xiaojun, CAO Zhenglin, et al. Formation conditions and exploration direction of large and medium gas reservoirs in the Junggar Basin, NW China. Petroleum Exploration and Development, 2020, 47(2): 247–259.

[2] YU Hongzhou. Development characteristics and genetic model of volcanic reservoir in complex tectonic belt of Hashan Area, northwestern margin of Junggar Basin. Petroleum Geology and Recovery Efficiency, 2019, 26(3): 46–53.

[3] ABLIMITI Yiming, ZHA Ming, YANG Fan, et al. Carboniferous igneous reservoir distribution and its controlling factors in Mahu-Dabasong Area, Junggar Basin. Xinjiang Petroleum Geology, 2019, 40(5): 564–569.

[4] MORAD S, KETZER M, DEROS L F. Spatial and temporal distributions of diagenetic alterations in siliciclastic rocks. Sedimentology, 2000, 47(1): 95–120.

[5] RASMUSSEN B, KRAPEZ B. Evidence of hydrocarbon and metalliferous fluid migration in the Palaeoproterozoic Earaheedy Basin of Western Australia. Journal of the Geological Society, 2000, 157(2): 355–366.

[6] PACKARD J, AL-AASM I S, SAMSON I, et al. A devonian “hydrothermal” chert reservoir: The 225 Bcf Parkland Field, British Columbia, Canada. AAPG Bulletin, 2001, 85(1): 51–84.

[7] BOLES J R, EICHHUBL P, GARVEN G, et al. Evolution of a hydrocarbon migration pathway along basin-bounding faults: Evidence from fault cement. AAPG Bulletin, 2004,

88(7): 947–970.

[8] HU Wenxuan, JIN Zhijun, ZHANG Yijie, et al. Mineralogy and geochemical records of episodic reservoiring of hydrocarbon: Example from the reservoirs in the northwest margin of Junggar Basin. Oil & Gas Geology, 2006, 27(4): 442–450.

[9] JIN Z, CAO J, HU W, et al. Episodic petroleum fluid migration in fault zones of the northwestern Junggar Basin (northwest China): Evidence from hydrocarbon-bearing zoned calcite cement. AAPG Bulletin, 2008, 92(9): 1225–1243.

[10] CAO J, JIN Z, HU W, et al. Improved understanding of petroleum migration history in the Hongche fault zone, northwestern Junggar Basin (northwest China): Constrained by vein-calcite fluid inclusions and trace elements. Marine and Petroleum Geology, 2010, 27(1): 61–68.

[11] LIN Huixi, MENG Fanchao, XU Youde, et al. Genesis of calcite veins in Carboniferous-Permian volcanic fractures, northwestern Junggar Basin. Chinese Journal of Geology, 2016, 51(3): 824–834.

[12] MUCHEZ P H, SLOBODNIK M, VIAENE W A, et al. Geochemical constraints on the origin and migration of paleofluids at the northern margin of the Variscan foreland, southern Belgium. Sedimentary Geology, 1995, 96(3): 191–200.

[13] CONTI A, TURPIN L, POLINO R, et al. The relationship between evolution of fluid chemistry and the style of brittle deformation: Examples from the Northern Apennines (Italy). Tectonophysics, 2001, 330(1): 103–117.

[14] BARKER S L, COX S F, EGGINNS S M, et al. Microchemical evidence for episodic growth of antitaxial veins during fracture-controlled fluid flow. Earth and Planetary Science Letters, 2006, 250(2): 331–344.

[15] MARFIL R, CAJA M A, TSIGE M, et al. Carbonate-cemented stylolites and fractures in the Upper Jurassic limestones of the eastern Iberian Range, Spain: A record of palaeofluids composition and thermal history. Sedimentary Geology, 2005, 178(4): 237–257.

[16] CAO Jian, HU Wenxuan, YAO Suping, et al. Carbon, oxygen and strontium isotope composition of calcite veins in the Carboniferous to Permian source sequences of the Junggar Basin: Implications on petroleum fluid migration. Acta Sedimentologica Sinica, 2007, 25(5): 722–729.

[17] LIU Yong, YUAN Haifeng, GAO Yao, et al. Genetic mechanism of calcite veins in Carboniferous-Permian volcanic reservoirs in the Hashan Area, Junggar Basin and its petroleum geological significance. Acta Geologica Sinica, 2017, 91(11): 2573–2583.

[18] LI Jun, TANG Yong, WU Tao, et al. Overpressure origin and its effects on petroleum accumulation in the conglomerate oil province in Mahu Sag, Junggar Basin, NW China. Petroleum Exploration and Development, 2020, 47(4): 679–690.

[19] CHEN Xin, LU Huafu, SHU Liangshu, et al. Study on tectonic evolution of Junggar Basin. Geological Journal of China Universities, 2002, 8(3): 257–267.

[20] HE Dengfa, ZHOU Lu, WU Xiaozhi. Occurrence and evolution of paleo-uplift and petroleum accumulation in Junggar Basin. Beijing: Petroleum Industry Press, 2012: 117.

[21] WU Kongyou, QU Jianhua, WANG Hehua. Strike-slip characteristics, forming mechanisms and controlling reservoirs of Dazhuluogou Fault in Junggar Basin. Journal of China University of Petroleum (Edition of Natural Science), 2014, 38(5): 41–47.

[22] CHEN Shi, GUO Zhaojie, QI Jiafu, et al. Three-stage strike-slip fault systems at northwestern margin of Junggar Basin and their im-plications for hydrocarbon exploration. Oil & Gas Geology, 2016, 37(3): 322–331.

[23] HE Dengfa, WU Songtao, ZHAO Long, et al. Tectonodepositional setting and its evolution during Permian to Triassic around Mahu Sag, Junggar Basin. Xinjiang Petroleum Geology, 2018, 39(1): 35–47.

[24] CHEN Gangqiang, ABLIMITI Yiming, BAI Lei, et al. Petroleum accumulation field in the deep strata of the eastern slope area of the Mahu Sag, Junggar Basin. Journal of Southwest Petroleum University (Science & Technology Edition), 2013, 35(6): 31–38.

[25] LIU Y S, HU Z C, GAO S, et al. In situ analysis of major and trace elements of anhydrous minerals by LA-ICP-MS without applying an internal standard. Chemical Geology, 2008, 257(1/2): 34–43.

[26] AL-AASM I S, TAYLOR B E, SOUTH B E. Stable isotope analysis of multiple carbonate samples using selective acid extraction. Chemical Geology (Isotope Geoscience), 1990, 80: 119–125.

[27] AL-AASM I S, MUIR I, MORAD S. Diagenetic conditions of fibrous calcite vein formation in black shales: Petrographic and chemical evidence. Canadian Journal of Petroleum Geology, 1993, 41: 46–56.

[28] HU Wenxuan, CHEN Qi, WANG Xiaolin, et al. REE models for the dis-crimination of fluids in the formation and evolution of dolomite reservoirs. Oil & Gas Geology, 2010, 31(6): 810–818.

[29] GAO Jian, HE Sheng, HE Zhiliang, et al. Genesis of calcite vein and its implication to petroleum preservation in Jingshan region, Mid-Yangtze. Oil & Gas Geology, 2014, 35(1): 33–41.

[30] MASUDA A, NAKAMURA N, TANAKA T. Fine structures of mutually normalized rare-earth patterns of chondrites. Geochimica et Cosmochimica Acta, 1973, 37(2): 239–248.

[31] LI Rongqing. Rare earth element distribution and its genetic signification of calcite in Hunan polymetallic metallogenic province. Journal of Mineralogy and Petrology, 1995, 15(4): 72–77.

[32] SCHMID S, WORDEN R, FISHER Q. Diagenesis and reservoir quality of the Sherwood Sandstone (Triassic), Corrib Field, Slyne Basin, west of Ireland. Marine and Petro-

leum Geology, 2004, 21(3): 299–315.

[33] XI K, CAO Y, LIN M, et al. Applications of light stable isotopes (C, O, H) in the study of sandstone diagenesis: A review. Acta Geologica Sinica, 2019, 93(1): 213–226.

[34] HAYES M J, BOLES J R. Evidence for meteoric recharge in the San Joaquin Basin, California, provided by isotope and trace element geochemistry. Marine and Petroleum Geology, 1993, 10(2): 135–144.

[35] KLINKHAMMER G P, ELDERFIELD H, MITRA A. Geochemical implications of rare earth element patterns in hydrothermal fluids from mid-ocean ridges. Geochimica et Cosmochimica Acta, 1994, 58(23): 5105–5113.

[36] SHAN Xiang, GUO Huajun, ZOU Zhiwen, et al. Diagenesis in alkaline environment and its influences on reservoir quality: A case study of middle-lower Permian clastic reservoirs in northwestern margin of Junggar Basin. Xinjiang Petroleum Geology, 2018, 39(1): 55–62.

[37] ZHOU Lu, ZHENG Jinyun, LEI Dewen, et al. Recovery of eroded thickness of the Jurassic of Chemo palaeouplift in Junggar Basin. Journal of Palaeogeography, 2007, 9(3): 243–252.

[38] ZHOU Yongshui, QIU Nansheng, SONG Xinying, et al. Study of source rock thermal evolution in over pressure formations in the hinterland of Junggar Basin. Chinese Journal of Geology, 2014, 49(3): 812–822.

[39] ZHANG Yijie, CAO Jian, HU Wenxuan. Timing of petroleum accumulation and the division of reservoir-forming assemblages, Junggar Basin, NW China. Petroleum Exploration and Development, 2010, 37(3): 257–262.

[40] FAN Cunhui, QIN Qirong, QIN Zhangjin. Volcanic rock reservoir identification and prediction: A case study of Carboniferous volcanic rocks in Zhongguai Swell in northwestern margin of Junggar Basin. Beijing: Science Press, 2016: 161–162.